

# Directed Oxygen Gradients Initiate a Robust Early Remodeling Response in Engineered Vascular Grafts

Marc Moore, PhD,<sup>1</sup> Ruben Moore, BS,<sup>2</sup> and Peter S. McFetridge, PhD<sup>1</sup>

Whereas functionally different, both organogenesis and wound-healing processes create zones or regions of hypoxia that persist until capillary networks are formed to facilitate oxygen and nutrient delivery. Similarly, regenerative processes within *in vitro* engineered tissues experience the same hypoxic regions, but without the capacity to form functional capillaries resulting in a major limitation in developing full-thickness organs and tissues. Due to the importance of oxygen in wound healing and tissue regeneration, we hypothesize that directed oxygen gradients can be used to modulate cell function and promote more effective tissue regeneration. The effect of controlled oxygen gradients on human smooth muscle cells (SMCs) was assessed using dual chambered perfusion bioreactors to regulate transport conditions occurring in a model vascular construct. SMCs were seeded onto the abluminal surface of the scaffold and cultured for 21 days under 3 independent gas environments: (1) 21% oxygen, (2) 11% oxygen, or (3) an ablumen to lumen oxygen gradient from 11% to 21%. When compared to 21% oxygen and 11% oxygen conditions, the directed 11%–21% oxygen gradient resulted in a raised metabolic activity and significantly improved cell migration. After 21 days from seeding, cells were shown to migrate entirely across the scaffold to the vessel lumen (>450  $\mu\text{m}$ ). Concomitant with a more uniform cell dispersion, scaffold mechanics were significantly enhanced with increased stiffness and tensile strength. Native oxygen gradients are known to play a pivotal role during organ development; these results show that directed oxygen gradients within *in vitro* systems can be used to facilitate early remodeling leading to significantly enhanced cell migration and scaffold biomechanics.

## Introduction

**M**OLECULAR OXYGEN PLAYS an important role in cell signaling as well as respiration, both of which directly affect cell behavior. Oxygen gradients exist throughout the body with blood oxygen levels varying regionally throughout the circulatory system and as a function of linear distance from the blood supply, resulting in zone-specific cell phenotypes.<sup>1,2</sup> In developing tissues and organs, hypoxic regions promote endothelial cells to stimulate angiogenesis, while normoxic regions inhibit angiogenic responses.<sup>3</sup> Understanding the effect of oxygen concentrations and gradients, within engineered tissue constructs during *in vivo* and *in vitro* maturation, is important due to the direct effects that modulate the cell behavior and phenotype.<sup>1,4</sup>

Physiological oxygen gradients have been studied for decades, with the first analytical measurements of oxygen levels in the microcirculation networks being made over 40 years ago.<sup>5</sup> Since then, the scientific understanding of oxygen transport has expanded from an initial view that oxygen gradients only occur in capillaries and organs to a more

complex understanding that oxygen can diffuse from blood to any surrounding tissue given a sufficient gradient.<sup>6</sup> The gold standard for understanding and predicting both longitudinal and radial oxygen gradients is the Krogh cylinder model, which determines the availability of oxygen in a given region of tissue to quantify the rate of cellular consumption.<sup>7</sup> Supporting these quantitative assessments, mathematical modeling of cellular nutrient consumption has shown that oxygen is most commonly expected to be the rate-limiting nutrient during the regenerative processes of construct development.<sup>8,9</sup> Additionally, empirical evidence has shown that oxygen is the limiting nutrient due to its low solubility in cell culture media and high consumption rate by cells.<sup>9</sup>

In addition to oxygen being a critical nutrient required for basic cell function, hypoxia is also an important physiological signal in the early stages of wound healing and angiogenesis.<sup>10</sup> Hypoxic preconditioning without the use of controlled gradients, where the entire system is under lowered O<sub>2</sub> conditions, has previously been used to enhance angiogenic capacity,<sup>11,12</sup> as well having been shown to

<sup>1</sup>J. Crayton Pruitt Family Department of Biomedical Engineering, University of Florida, Gainesville, Florida.

<sup>2</sup>Department of Chemical Engineering, University of Florida, Gainesville, Florida.

enhance the mechanical properties of engineered heart valves.<sup>13</sup> Whereas the exact mechanisms that induce these changes are not fully understood, hypoxia has been shown to speed the rate of collagen synthesis in cultured fibroblasts and to enhance fibrin remodeling *in vitro*.<sup>14,15</sup> The cellular response to hypoxia is primarily mediated by the Hypoxia Inducible Factor 1- $\alpha$  (HIF1- $\alpha$ ) and additionally by a variety of reactive oxygen species.<sup>16</sup> For example, in the presence of a hypoxic environment, the HIF1- $\alpha$  pathway upregulates TGF- $\beta$ 1, which plays an important role in fibrin remodeling as well as cell growth, proliferation, differentiation, and apoptosis.<sup>14,17-19</sup> Under the same hypoxic environment, the HIF1- $\alpha$  pathway is also responsible for increased PDGF expression, which has been shown to direct the migration, differentiation, and function of many cell types during development.<sup>20</sup>

*In vivo*, molecular oxygen exists in gradients rather than discrete hypoxic and normoxic zones. Polymeric scaffolds cultured under static conditions have shown oxygen concentration gradients ranging from 175 to 22  $\mu$ M, which has been shown to correlate with cell density and viability.<sup>4</sup> Additionally, oxygen gradients applied to cell monocultures have shown correlating regional variation in protein expression.<sup>1</sup> Thus, it was hypothesized that oxygen gradients play a significant role regulating early remodeling events, where limited porosity and the lack of a functional capillary system compound mass transfer limitations and inhibit regenerative processes.

The goal of these investigations was to utilize discrete perfusion zones within a dual perfusion bioreactor system to generate directed oxygen gradients across an engineered vascular construct, with an aim to speed cell migration, improve cell distribution, and activate remodeling by augmenting extracellular matrix (ECM) synthesis. To accomplish this, human smooth muscle cells (SMCs) were seeded onto the abluminal surface of a model vascular scaffold derived from the human umbilical vein (HUV),<sup>21</sup> and 3 independent gas environments were assessed: (1) ablumen and lumen circuits maintained at 11% oxygen, (2) ablumen and lumen circuits maintained at 21% oxygen, and (3) an applied gradient generated by maintaining the ablumen at 11% oxygen and lumen at 21% (11%:21% oxygen gradient). After 3 weeks of culture, analysis included histology, cellular proliferation and metabolism, and mechanical analysis.

## Materials and Methods

### HUV dissection

Investigations herein conform to the principles outlined were approved by the University of Florida Institutional Review Board (approval #64-2010) in concert with the Declaration of Helsinki for use of human tissue or subjects. Placentas from full-term deliveries were collected from the University of Florida Shands Hospital (Gainesville, FL) within 4 h of delivery. HUV sections were dissected using an automated method as previously described.<sup>21</sup> Briefly, 100-mm segments of human umbilical cords (<24 h from delivery) were collected and mounted onto stainless steel mandrels and frozen to  $-80^{\circ}\text{C}$  overnight. Frozen vessels were then loaded into a 10" CNC bench lathe (MicroKinetics, Kennesaw, GA), and cut to a wall thickness of 750  $\mu$ m at a rotational speed of 2800 RPM with an axial cutting rate of

5 mm/s. Lathed cords were then progressively thawed to  $5^{\circ}\text{C}$  over 4 h before decellularization.

### Decellularization and lyophilization

Dissected HUV samples were placed into a 100 mL KI-MAX media storage bottles containing a 1% SDS (Thermo Scientific, Rockford, IL) solution with phosphate-buffered saline (PBS) to obtain a solvent/tissue mass of 20:1 (w:v), which was then put on an orbital shaker plate at 100 rpm for 24 h. Samples were then rinsed with PBS at 30-min, 1-, 3-, 6-, 12-, and 24-h intervals before incubation overnight at  $37^{\circ}\text{C}$  in a 70 U/mL DNase I solution (Sigma-Aldrich, St. Louis, MO) in PBS with pH 7.4. Samples were rinsed using the same protocol as above, then terminally sterilized using a 0.2% peracetic acid/4% ethanol (Sigma-Aldrich) solution for 2 h, and finally pH balanced (7.4) using multiple washes of PBS.

Following decellularization, 4-mm-diameter silicon tubing was inserted through the HUV scaffolds lumen to maintain a uniform tubular shape during the lyophilization process. Mounted scaffolds were prefrozen to  $-85^{\circ}\text{C}$  before lyophilization using a Millrock Bench-Top Freeze Dryer Model BT85A (Kingston, NY) for 24 h at  $-85^{\circ}\text{C}$  under 10 mT vacuum.

### Cell culture and seeding

Human SMCs (CRL 2854) were used between passages 5 and 10 (ATCC, Manasses, VA) and cultured under standard conditions at  $37^{\circ}\text{C}$  and 5%  $\text{CO}_2$ . Cells were detached from cell culture plates using Accutase (Thermo Scientific, Waltham, MA), centrifuged, and resuspended in culture media to a final concentration of 4 million cells/mL. Cells were then seeded directly onto the 10-cm-long decellularized, lyophilized HUV scaffolds via direct pipetting of 1.5 mL of the cell solution onto the scaffold at a cell density of  $6 \times 10^5$  cells/linear cm. To verify the uniformity of this seeding technique, preliminary experiments were performed. Briefly, 5-mm tubular ringlets of the seeded constructs were cut open to form flat sheets, and then stained with Calcein AM (Invitrogen, Carlsbad, CA). Fluorescence microscopy was used to image live cells on the abluminal surface of the scaffold. Uniformity of cell seeding was assessed with ImageJ by quantifying the average distance between adjacent cells within random, representative 500- $\mu\text{m}^2$  regions, and then comparing regions along the surface of the construct. Additionally, 5-mm-long sections of the cell-seeded tubules were analyzed for the total initial DNA content using the Pico green assay (Invitrogen), and evaluated to ensure a uniform DNA content between the sections. Despite a degree of variation in the surface population that occurred based on a statistical error, average cell density calculations indicate uniform seeding on the surface of the construct. All samples were incubated in standard culture media consisting of the high-glucose Dulbecco's Modified Eagle's Medium (DMEM; HyClone, Rockford, IL), supplemented with 10% FBS (Gibco, Carlsbad, CA), for 1 day before insertion into the perfusion bioreactors.

### Bioreactor setup and conditions

Cell-seeded tubular constructs were cultured in the dual perfusion bioreactors (Fig. 1A, B) for 3 weeks with a luminal flow rate of 30 mL/min and pulse rate of 60 BPM. With the exception of variable  $\text{O}_2$  concentrations, the environment

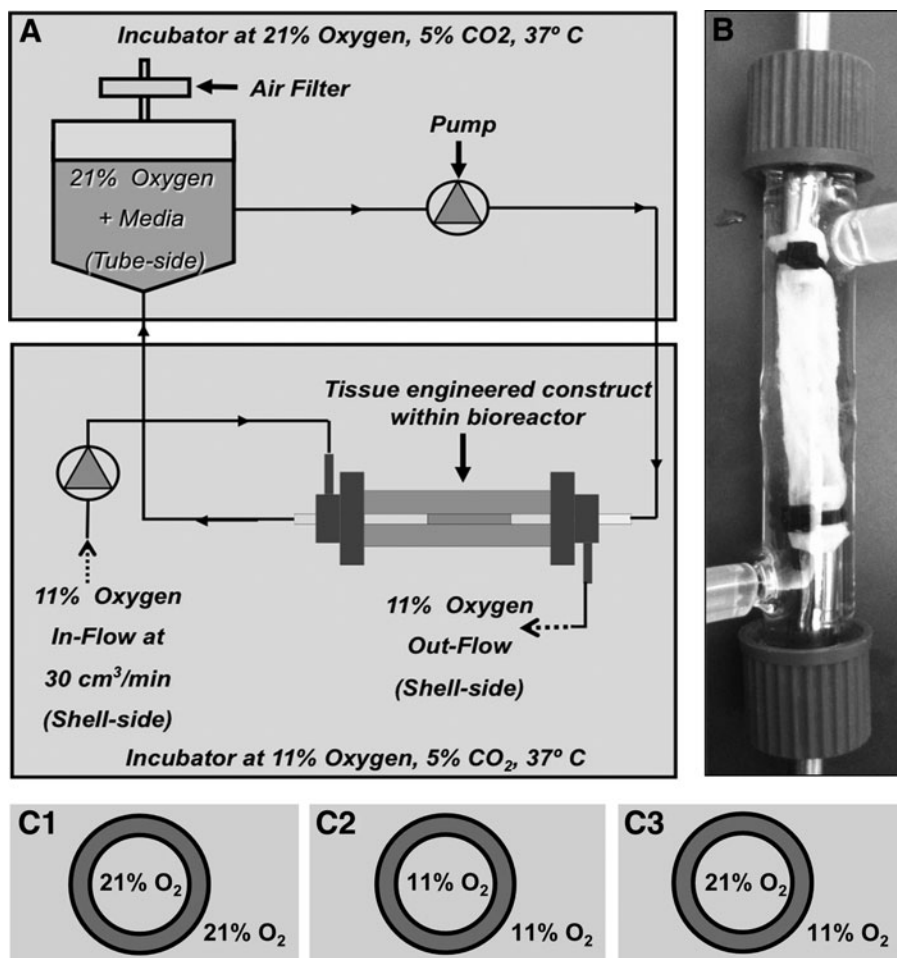


**FIG. 1.** Bioreactor process flow, culture conditions, and scaffold preparation used to study the effects of an oxygen gradient in a perfusion bioreactor (A). The decellularized human umbilical vein scaffold was lyophilized and cells were seeded on the ablumen and cultured in perfusion bioreactors (B) for 21 days. Scaffolds were subjected to the conditions shown in (C1–C3).

was maintained under standard cell culture conditions of 37°C and 5% CO<sub>2</sub>. Pressure levels on both the abluminal and luminal sides of the scaffold were maintained at negligible levels (<2 mmHg) and normalized to prevent the formation of a pressure gradient across the scaffold. To avoid shearing cells off of the bioscaffold during initial adhesion, the initial flow rate of 10 mL/min was progressively increased by 5 mL/min each day, until day 5, when the flow rate reached 30 mL/min and was maintained for a total culture period of 21 days. Abluminal and luminal average flow velocities were 0.0025 m/s. Glucose levels were maintained at 4.5 g/L during the cell culture period. Three conditions were assessed: (1) both ablumen and lumen maintained at an 11% oxygen, (2) both ablumen and lumen maintained at a 21% oxygen, and (3) the ablumen maintained at an 11% oxygen and lumen at 21% (11%:21% oxygen gradient) (Fig. 1C1–C3). In all conditions, media were perfused only through the lumen with the ablumen O<sub>2</sub> in a gas state, see Figure 1. Analysis of PO<sub>2</sub> levels in cell culture media under standard atmospheric oxygen conditions (21%) was assessed using a Nova Biomedical Bioprofile 400 System (Waltham, MA). At atmospheric levels, PO<sub>2</sub> was found to be 181 ± 12 mmHg and at 11% O<sub>2</sub> conditions 68.2 ± 3.38 mmHg. Culture media in the bioreactor were replenished every 2 days.

After 21 days perfusion culture, the 10-cm-long tubular scaffolds were dissected into 5-mm ringlets. Ringlets from the distal, proximal, and central regions of each construct

were distributed between mechanical, histological, and cellular analysis to account for regional variation within the tubular scaffolds ( $n=3$  for each bioreactor and 3 bioreactors were analyzed for each condition).

#### Histology

Masson's Trichrome Staining (Sigma-Aldrich) and Hematoxylin and Eosin (H&E; Richard-Alan Scientific, Kalamazoo, MI) staining protocols were used for histology. Using a Microm HM550 cryostat (Thermo Scientific), tissue ringlets were embedded in the Neg-50 freezing medium (Thermo Scientific), and then sectioned into 7- $\mu$ m-thick sections with the cutting edge perpendicular to the length of the ringlets. Sections were fixed, stained, dehydrated, using standard conditions, and then images captured using an Imager Zeiss M2 light epifluorescent microscope and a Zeiss Axiocam HRm digital camera (Carl Zeiss MicroImaging, Thornwood, NY). Samples were stained using SYTO RNA-Select (Invitrogen) for further verification of cell migration and an indirect assessment of viability.

#### Mechanical analysis

Tensile properties were assessed using an Instron uniaxial tensile testing rig (Model 5544; Canton, MA) equipped with a 50 N static load cell capable of a force resolution  $\geq 0.0125$  N (Model 2530-437; Instron). Scaffold specimens were cut into

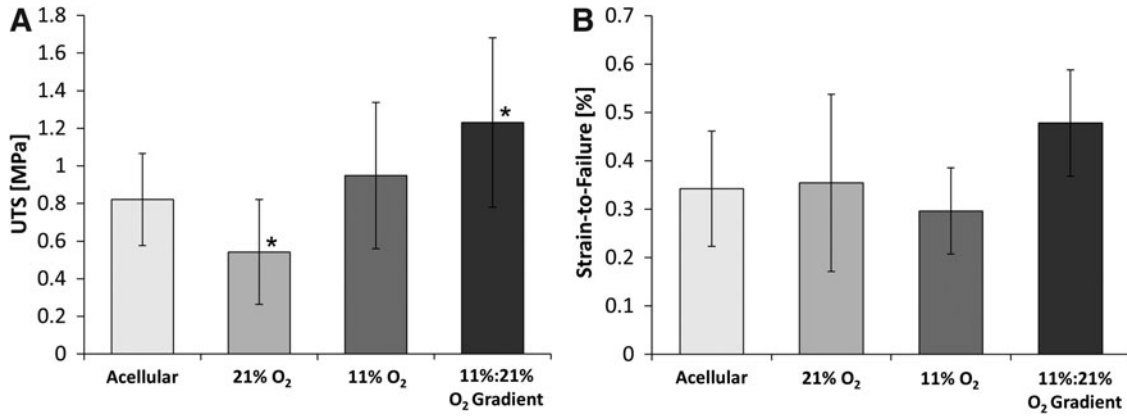


**FIG. 2.** Mechanical analysis of constructs after 21 days of perfusion culture, including the ultimate tensile strength (UTS) (A) and the strain at failure (B). Asterisks (\*) indicate that the Tukey’s test found the results to be statistically significant between two groups at  $p < 0.05$ .  $n = 6$ .

3-mm-wide ringlets ( $n = 6$ ), and then loaded using stainless steel hooks (as shown in Fig. 4A). Samples were preloaded to a stress of 0.05 N, and then progressively tensioned until failure at a constant rate of 5 mm/min. Load and displacement values were recorded over time, and then used to calculate the stress–strain values.

Strain values were calculated using the equation  $\epsilon = \frac{L_F - L_I}{L_I}$  in which, the sample deformation ( $L_F - L_I$ ) is divided by the initial length  $L_I$ , where  $L_F$  is the extension at failure. The engineering stress values for the ringlets were calculated using the equation  $\sigma = \frac{F}{(2tw)}$ , where  $t$  is the thickness of the samples,  $w$  is the width,  $F$  is the normal force, and  $2tw$  is the

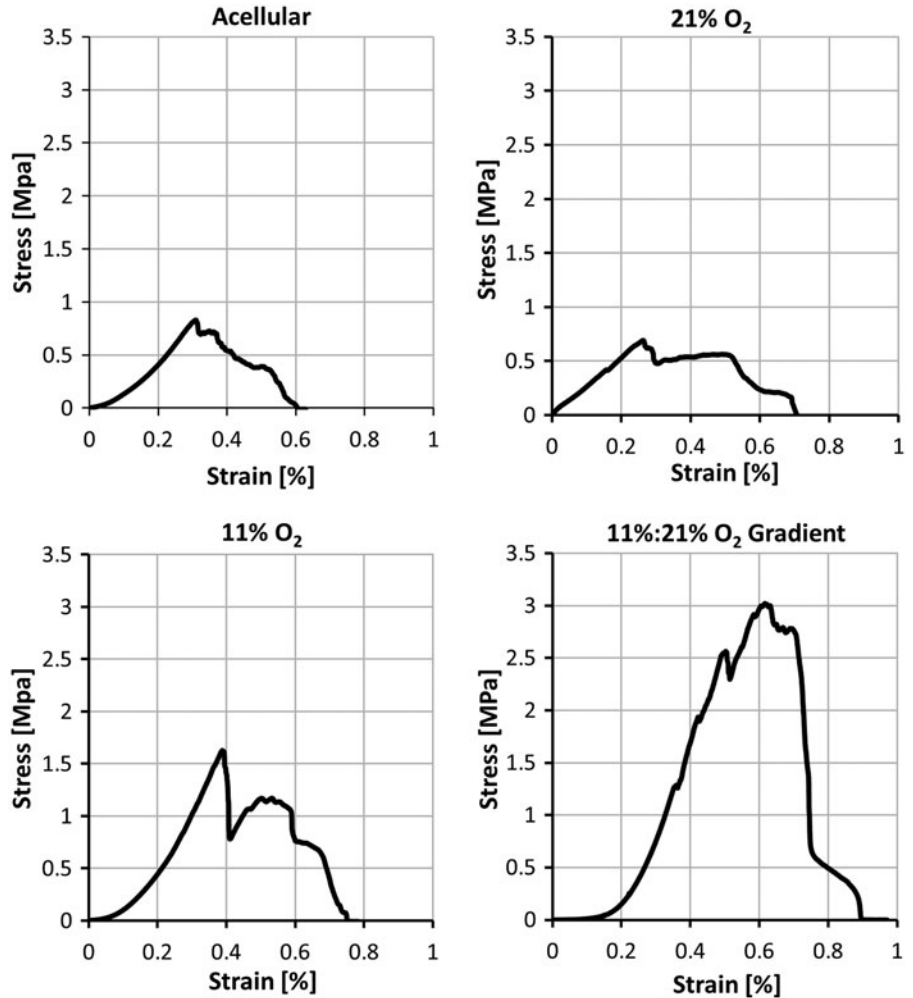


**FIG. 3.** Representative stress–strain curves of constructs after 21 days perfusion culture under 21% oxygen, 11% oxygen, and gradient conditions from the ablumen to the lumen of 11% to 21% oxygen.

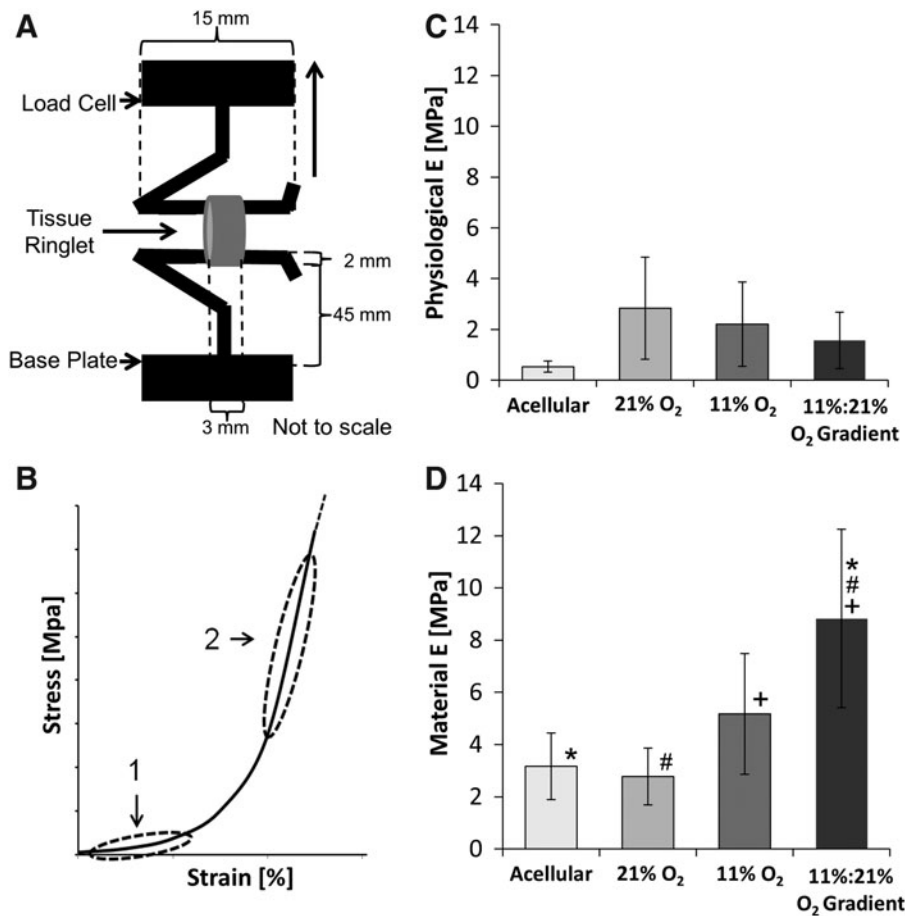


**FIG. 4.** Physiological and material elastic moduli after 21 days culture. A tensile testing rig (**A**) was used to determine the physiological moduli, shown as region 1 in (**B**), and the material moduli shown as region 2 in (**B**). Physiological moduli (**C**) were determined by finding the slope of the linear region between 10.6 kPa (80 mmHg) and 16.0 kPa (120 mmHg). Material moduli values (**D**) are highest in controlled oxygen gradient conditions. Asterisks, hash marks, and plus signs (\*, #, and +) indicate that the Tukey's test found the results to be statistically significant between two groups at  $p < 0.05$ .  $n = 6$ .

cross-sectional area of the ringlet. The final thickness of the samples  $t$  was measured to be  $\pm 625 \mu\text{m}$ . The elastic moduli of the constructs, calculated as  $(\sigma/\epsilon)^{22}$  were assessed over two regions: a high-strain region (material modulus), and a low-strain region ranging from 10.6 kPa (80 mmHg) to a maximum of 16.0 kPa (120 mmHg) that reflects physiologic behavior (physiological modulus).<sup>23,24</sup>

#### Cell proliferation and metabolism

Samples were weighed, and then the cell metabolism capability was quantified using an AlamarBlue (AB; Invitrogen) assay, where the fluorescence was measured at 530–560 nm excitation and 590 nm emission wavelength after a 2-h incubation at 37°C and 5% CO<sub>2</sub>. Final values were given as the percent reduction (AB) per million cells for each sample. Following this nondestructive cellular assay, DNA per gram of tissue was quantified using the PicoGreen (Invitrogen) assay as per the manufacturer's instructions. An average of 6 pg DNA per cell was determined experimentally and results were represented as cells/mg tissue.

#### Cell migration

Cell migration data were collected using computer software to localize the cell location by analyzing H&E stained sections. For each ringlet,  $5 \times 7\text{-}\mu\text{m}$  sections were collected with a distance of 20  $\mu\text{m}$  between each consecutive slice and stained with H&E. Images were taken at a magnification of

$5 \times$  using a light microscope, and then each section was analyzed for cell migration using the measurement function of ImageJ Version 1.45s software (NIH, Bethesda, MD). The maximum migration distance was calculated as the shortest perpendicular distance from the abluminal surface (seeded surface) to the leading edge of cell migration. As shown in Figure 5, the leading edge was defined as a line connecting cells that had migrated the farthest from the cell-seeded abluminal surface. Five measurements of the maximum migration distance were made on each section with a total of 25 values per sample, which were then averaged.

#### Statistics

Results are reported as mean  $\pm$  standard deviation. Data analysis was performed using SPSS (IBM, Somers, NY). To determine differences between time points for each sample type, a one-way analysis of variance (ANOVA) was performed to determine the statistical significance ( $p < 0.05$ ) within each data set. When the ANOVA detected significance, a Tukey's multiple comparison test was run at a 95% confidence level.

## Results

### Mechanical analysis

Tensile analysis of constructs cultured under the 11%:21% oxygen gradient conditions show significant increases in

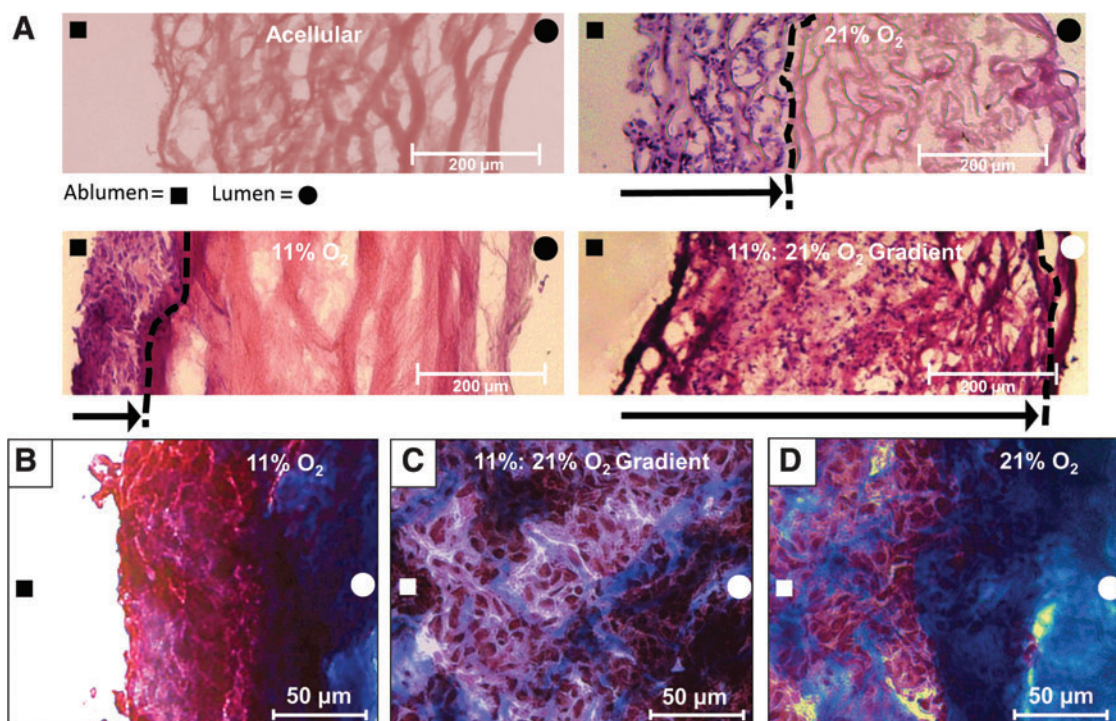


**FIG. 5.** Histological image analysis. Human smooth muscle cells were seeded on the abluminal surface and cultured under specified perfusion conditions for 21 days. **(A)** Hematoxylin and eosin stained sections show cell migration across the scaffold as a function of each respective gas condition. These data show constructs cultured using controlled  $O_2$  gradients to have increased cell migration relative to all other conditions. **(B)** Masson's Trichrome staining was used to assess collagen and ECM fiber alignment within the remodeled zone. Constructs cultured under 11%  $O_2$  conditions displayed dense regions of amorphous collagen fibers (blue) at the leading edge of the migration front with reduced fiber deposition between densely packed cells (red). Under these hypoxic conditions, cells were predominantly localized within 50–100  $\mu\text{m}$  of the seeded surface. **(C)** Under 11%:21%  $O_2$  gradient conditions, cells migrated across the bulk scaffold and appear more disperse relative to other conditions. No specific fiber alignment or structure was noted. **(D)** Results from the 21%  $O_2$  samples were similar to the 11%  $O_2$  conditions, displaying a leading edge of cell migration that reached the  $\sim 250$ – $300$   $\mu\text{m}$  from the seeded surface, with dense regions of amorphous collagen fibers (blue) at the lead edge. The distance of cell migration from the abluminal surface is shown by an arrow, " $\rightarrow$ ", pointing from the abluminal surface, indicated by " $\blacksquare$ ", to the leading edge of cell migration, indicated by a "—" line, with the luminal side indicated by " $\bullet$ ". Color images available online at [www.liebertpub.com/tea](http://www.liebertpub.com/tea)

both the elastic modulus and ultimate tensile stress (UTS). Gradient-cultured constructs displayed an ultimate tensile strength of  $1.23 \pm 0.45$  MPa relative to normoxic (21%) and hypoxic (11%)  $O_2$  conditions resulting in UTS of  $0.54 \pm 0.28$  MPa and  $0.95 \pm 0.39$  MPa, respectively (Fig. 2). Strain-to-failure values increased 0.21% in gradient-cultured constructs in comparison to those cultured using 11%  $O_2$ .

Unlike native vessels with a biphasic stress–strain response curve, the tensile analysis represented in Figure 3 shows constructs cultured under normoxic conditions to display a more linear response without any significant toe region. By contrast, constructs cultured in 11%  $O_2$  conditions had a more defined toe region occurring until 0.1% strain and those cultured in an oxygen gradient had a progressively larger toe region occurring until 0.2% strain. The highest material elastic modulus of  $8.83 \pm 3.41$  MPa, was from the constructs cultured under the oxygen gradient in comparison to using normoxic conditions ( $2.78 \pm 1.09$  MPa) and 11%  $O_2$  conditions ( $5.17 \pm 2.31$  MPa) (Fig. 4). Trends indicate that the physiological modulus in normoxic conditions, at  $2.83 \pm 2.01$  MPa, was highest and similar to the material modulus despite lacking statistical significance at  $p < 0.05$ . Physiological modulus was lowest in oxygen gradient con-

ditions at  $1.56 \pm 1.11$  MPa followed by 11%  $O_2$  conditions at  $2.20 \pm 1.66$  MPa (Fig. 4).

#### Histology and cell migration

H&E staining of constructs shows significant differences in cell migration through the scaffold for each culture condition (Fig. 5A). Constructs cultured under 21%  $O_2$  conditions had more cell migration from the abluminal surface than constructs cultured under 11%  $O_2$  conditions, which had accumulation of a cell mass on the surface. In contrast, constructs cultured under an 11%:21% ablumen to lumen  $O_2$  gradient showed the most cell migration with cells reaching the luminal surface. Masson's Trichrome staining shows that constructs cultured under 11%  $O_2$  conditions had dense regions of amorphous collagen fibers at the leading edge of the migration front, and reduced fiber deposition between densely packed cells (red) (Fig. 5B). Under 11%:21%  $O_2$  gradient conditions, cells migrated across the bulk scaffold and were more disperse relative to other conditions. No specific fiber alignment or structure was noted (Fig. 5C). In samples cultured in 21%  $O_2$ , a dense region of amorphous collagen fibers (blue) was observed as the leading edge of cell migration

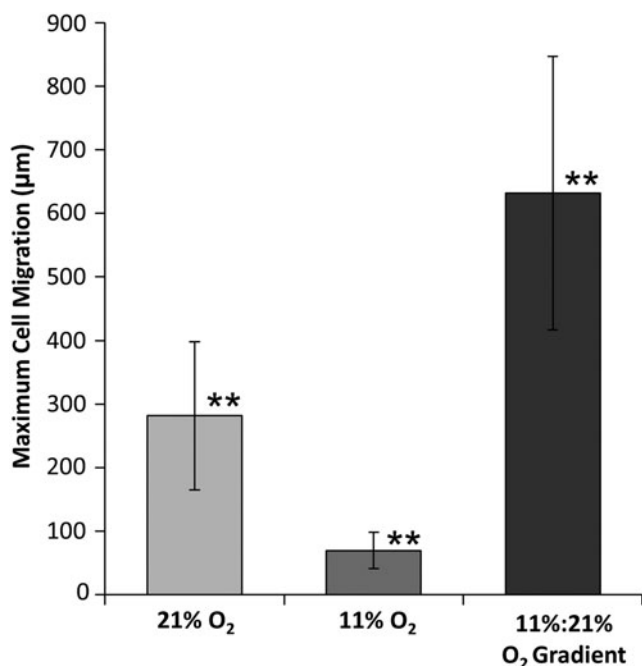


**FIG. 6.** Maximum cell migration distance was calculated as the average distance from the cell-seeded ablumen to the leading edge of cell migration. Double asterisks (\*\*) indicate that the Tukey's test found the results to be statistically significant between all groups at  $p < 0.05$ .  $n = 6$ .

(Fig. 5D). After 21 days, the maximum cell migration distance ( $632 \pm 215 \mu\text{m}$ ) occurred in constructs cultured under the defined oxygen gradient. Constructs cultured in 11% O<sub>2</sub> conditions had the least migration of  $69.3 \pm 28.6 \mu\text{m}$ , while those cultured in normoxic conditions had a migration of  $282 \pm 116 \mu\text{m}$  (Fig. 6). Additionally, RNA staining of constructs cultured with the directed oxygen gradient showed that cells migrated fully from the ablumen to the luminal surface and had a more flattened elongated morphology as they approached the luminal surface (Fig. 7).

#### Cell proliferation and metabolism

The concentration of cells/g tissue displayed no significant differences between samples with the highest density, at  $13.2 \pm 3.43$  million cells/mg tissue, and lowest in 11% O<sub>2</sub>-cultured samples, at  $10.1 \pm 5.49$  million cells/mg tissue. The metabolic activity of cells cultured under the directed gra-

dient conditions was  $32.6 \pm 11.8\%$  reduction AB/g tissue, which was significantly greater than cells in the 21% O<sub>2</sub> condition with  $8.87 \pm 2.91\%$  reduction AB/g tissue (Fig. 8).

#### Discussion

ECM remodeling during scaffold recellularization is a multifactorial process that effects not only cell functionality, but results in dynamic changes in the scaffold mechanical properties. It is clear that the chemotactic driving force during recellularization is a function of nutrient concentration, availability, and consumption, which are further functions of pressure and scaffold porosity. By modulating O<sub>2</sub> source/sink concentrations within dual-perfusion bioreactors, we have shown that controlled gradients directly modulate cell migration, scaffold modulus, ultimate tensile strength, and cell metabolic activity. Accordingly, these results further illustrate the potential to actively control ECM remodeling and cell phenotype to develop physiologically correct and biologically functional constructs.

These investigations show that regulation of the systems oxygen tension was an important factor in controlling scaffold mechanics. As in previous studies, these results show that constructs cultured in hypoxic conditions have both higher moduli and ultimate tensile strengths relative to constructs cultured in normoxic condition.<sup>13</sup> However, these investigations show that the use of a directed oxygen gradient offers further enhancement of remodeling activity that improves the materials modulus and tensile strength when compared to cultures in a constant low oxygen tension. Importantly, these results show enhanced cell migration in an *ex vivo* scaffold model that has historically been difficult to populate (*in vitro*), due largely to inadequate nutrient transport conditions.<sup>25–27</sup> In addition, comparing material moduli to physiological moduli, for each bioreactor condition, reveals a biphasic response as indicated by the formation of two defined regions, a toe region and a linear region, which was most distinct in constructs cultured using a directed oxygen gradient. Native blood vessels typically have large toe regions on their stress–strain curves due to their composite nature and high elastin content. While further studies need to be done to define changes in elastin composition, mechanical data indicate changes in the ECM composition and structure.<sup>28</sup>

Oxygen was most deficient in constructs cultured using 11% O<sub>2</sub> conditions and resulted in the least cell migration of all conditions. These 11% O<sub>2</sub> conditions further decreased the amount of available oxygen deep within the construct

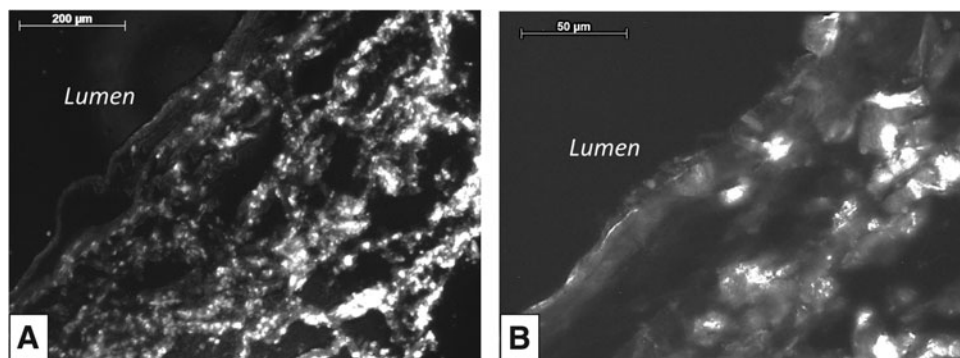
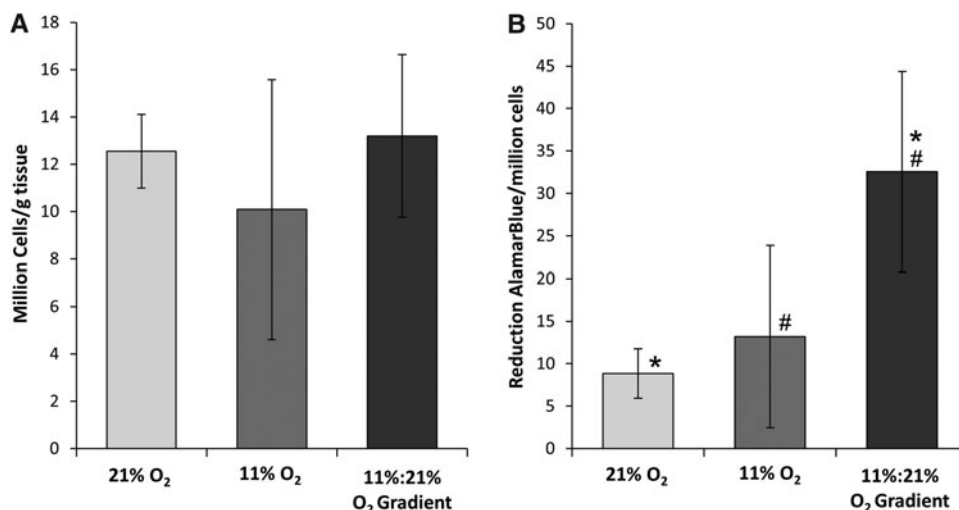


**FIG. 7.** Syto RNA staining of constructs cultured under 11%:21% oxygen gradient after 21 days in the bioreactor. Under an oxygen gradient, full scaffold migration occurred (A) and cells showed flattened morphology (B) as they approached the luminal surface. Scale bars = 200 µm in (A) and 50 µm in (B).

**FIG. 8.** The cell proliferation and metabolic activity of constructs cultured using each respective gas environment for 21 days. Asterisks and hash marks (\* and #) indicate that the Tukey's test found the results to be statistically significant between two groups at  $p < 0.05$ .  $n = 6$ .



resulting in cells remaining on the surface without significant migration. Twenty one percent O<sub>2</sub> were similar to 11% O<sub>2</sub> with a uniform and limited oxygen concentration available on both surfaces, which resulted in minimal cell migration no more than a few hundred microns into the construct.<sup>9</sup> The maximum cell migration distance occurred with the 11% to 21% oxygen gradient (cells were seeded on the surface exposed to the 11% O<sub>2</sub> atmosphere). This indicates that the mass transfer limitations are exacerbated in *ex vivo* derived scaffolds, can be overcome at least, in part, using chemotactic oxygen gradients to promote migration. While deficiencies in oxygen transport can be compensated by controlling oxygen gradients, ultimately, the formation of a vascular network is the long-term goal to sustain high cell densities and biological function.

In addition to showing that oxygen is an important modulator of cell migration and ECM remodeling, significant differences in cell metabolism were seen with respect to varying O<sub>2</sub> concentrations under perfusion conditions. While oxygen tension conditions did not significantly affect cell proliferation and final density, constructs cultured using the oxygen gradient had a higher metabolic activity than those cultured under either normoxic or hypoxic conditions. This trend occurs in conjunction with similar trends of increasing elastic moduli and UTS in constructs cultured in the oxygen gradient. It is well known that hypoxic environments cause downregulation of metabolic supply and demand of ATP, and thus, it is interesting that these results show that constructs cultured using a directed oxygen gradient had increased metabolic activity.<sup>29</sup>

It is particularly important to hasten *in vitro* construct regeneration to meet the clinical demand. However, if constructs are less than fully developed at implantation, physiological and biological stresses are more likely to result in poor biological integration leading to graft failure. This is particularly important in applications such as vascular bypass, where the lead-time for patient use is minimal, yet construct mechanics and biological functionality must be stringently maintained. In the early stages of *in vivo* development, zones of hypoxia provide a chemotactic signal that promotes cell migration and directs the cell phenotype that ultimately affects the constructs' biological and mechanical

properties.<sup>30</sup> In these investigations, the use of controlled and directed oxygen gradients *in vitro* significantly enhances the initial stages of construct maturation over environments with a globally lowered O<sub>2</sub> tension. This is especially important with scaffold materials derived from *ex vivo* tissues, where nutrient transport conditions directly inhibit cell migration. As such, a continued understanding of these key conditions may lead to enhanced implants with improved functionality and reduced timelines for clinical applications.

#### Acknowledgments

The authors are thankful for the financial support provided by the National Institute of Health (NIH R01 HL088207).

#### Disclosure Statement

No competing financial interests exist.

#### References

- Allen, J.W., and Bhatia, S.N. Formation of steady-state oxygen gradients *in vitro*: Application to liver zonation. *Biotechnol Bioeng* **82**, 253, 2003.
- Tsai, A.G., Johnson, P.C., and Intaglietta, M. Oxygen gradients in the microcirculation. *Physiol Rev* **83**, 933, 2003.
- Pugh, C.W., and Ratcliffe, P.J. Regulation of angiogenesis by hypoxia: role of the hif system. *Nat Med* **9**, 677, 2003.
- Radisic, M., Malda, J., Epping, E., Geng, W., Langer, R., and Vunjak-Novakovic, G. Oxygen gradients correlate with cell density and cell viability in engineered cardiac tissue. *Biotechnol Bioeng* **93**, 332, 2006.
- Duling, B.R., and Berne, R.M. Longitudinal gradients in periarteriolar oxygen tension. A possible mechanism for the participation of oxygen in local regulation of blood flow. *Circ Res* **27**, 669, 1970.
- Pittman, R.N. Oxygen gradients in the microcirculation. *Acta Physiol (Oxf)* **202**, 311, 2011.
- Krogh, A. The number and distribution of capillaries in muscles with calculations of the oxygen pressure head necessary for supplying the tissue. *J Physiol* **52**, 409, 1919.
- Devarapalli, M., Lawrence, B.J., and Madihally, S.V. Modeling nutrient consumptions in large flow-through



- bioreactors for tissue engineering. *Biotechnol Bioeng* **103**, 1003, 2009.
9. Martin, Y., and Vermette, P. Bioreactors for tissue mass culture: design, characterization, and recent advances. *Biomaterials* **26**, 7481, 2005.
  10. Falanga, V., Zhou, L., and Yufit, T. Low oxygen tension stimulates collagen synthesis and *coll1a1* transcription through the action of *tgf-beta1*. *J Cell Physiol* **191**, 42, 2002.
  11. Perez-Amodio, S., Tra, W.M., Rakhorst, H.A., Hovius, S.E., and van Neck, J.W. Hypoxia preconditioning of tissue-engineered mucosa enhances its angiogenic capacity *in vitro*. *Tissue Eng Part A* **17**, 1583, 2011.
  12. Griffith, C.K., and George, S.C. The effect of hypoxia on *in vitro* prevascularization of a thick soft tissue. *Tissue Eng Part A* **15**, 2423, 2009.
  13. Balguid, A., Mol, A., van Vlimmeren, M.A., Baaijens, F.P., and Bouten, C.V. Hypoxia induces near-native mechanical properties in engineered heart valve tissue. *Circulation* **119**, 290, 2009.
  14. Neidert, M.R., Lee, E.S., Oegema, T.R., and Tranquillo, R.T. Enhanced fibrin remodeling *in vitro* with *tgf-beta1*, insulin and plasmin for improved tissue-equivalents. *Biomaterials* **23**, 3717, 2002.
  15. Horino, Y., Takahashi, S., Miura, T., and Takahashi, Y. Prolonged hypoxia accelerates the posttranscriptional process of collagen synthesis in cultured fibroblasts. *Life Sci* **71**, 3031, 2002.
  16. Guzy, R.D., Hoyos, B., Robin, E., Chen, H., Liu, L., Mansfield, K.D., Simon, M.C., Hammerling, U., and Schumacker, P.T. Mitochondrial complex iii is required for hypoxia-induced ros production and cellular oxygen sensing. *Cell Metab* **1**, 401, 2005.
  17. Border, W.A., and Noble, N.A. Transforming growth factor beta in tissue fibrosis. *N Engl J Med* **331**, 1286, 1994.
  18. Letterio, J.J., and Roberts, A.B. Regulation of immune responses by *tgf-beta*. *Annu Rev Immunol* **16**, 137, 1998.
  19. Pollman, M.J., Naumovski, L., and Gibbons, G.H. Vascular cell apoptosis: cell type-specific modulation by transforming growth factor-beta1 in endothelial cells versus smooth muscle cells. *Circulation* **99**, 2019, 1999.
  20. Hoch, R.V., and Soriano, P. Roles of *pdgf* in animal development. *Development* **130**, 4769, 2003.
  21. Daniel, J., Abe, K., and McFetridge, P.S. Development of the human umbilical vein scaffold for cardiovascular tissue engineering applications. *ASAIO J* **51**, 252, 2005.
  22. Roeder, R., Wolfe, J., Lianakis, N., Hinson, T., Geddes, L.A., and Obermiller, J. Compliance, elastic modulus, and burst pressure of small-intestine submucosa (sis), small-diameter vascular grafts. *J Biomed Mater Res* **47**, 65, 1999.
  23. Amensag, S., and McFetridge, P.S. Rolling the human amnion to engineer laminated vascular tissues. *Tissue Eng Part C Methods* **18**, 903, 2012.
  24. Duprey, A., Khanafer, K., Schlicht, M., Avril, S., Williams, D., and Berguer, R. *In vitro* characterisation of physiological and maximum elastic modulus of ascending thoracic aortic aneurysms using uniaxial tensile testing. *Eur J Vasc Endovasc Surg* **39**, 700, 2010.
  25. Tosun, Z., Villegas-Montoya, C., and McFetridge, P.S. The influence of early-phase remodeling events on the biomechanical properties of engineered vascular tissues. *J Vasc Surg* **54**, 1451, 2011.
  26. Abousleiman, R.L., Reyes, Y., McFetridge, P., and Sikavitsas, V. The human umbilical vein: a novel scaffold for musculoskeletal soft tissue regeneration. *Artif Organs* **32**, 735, 2008.
  27. Moore, M., Sarntinoranont, M., and McFetridge, P. Mass transfer trends occurring in engineered *ex vivo* tissue scaffolds. *J Biomed Mater Res A* **100**, 2194, 2012.
  28. Roach, M.R., and Burton, A.C. The reason for the shape of the distensibility curves of arteries. *Can J Biochem Physiol* **35**, 681, 1957.
  29. Wheaton, W.W., and Chandel, N.S. Hypoxia. 2. Hypoxia regulates cellular metabolism. *Am J Physiol Cell Physiol* **300**, C385, 2011.
  30. Annabi, B., Lee, Y.T., Turcotte, S., Naud, E., Desrosiers, R.R., Champagne, M., Eliopoulos, N., Galipeau, J., and Beliveau, R. Hypoxia promotes murine bone-marrow-derived stromal cell migration and tube formation. *Stem Cells* **21**, 337, 2003.

Address correspondence to:

Peter S. McFetridge, PhD

J. Crayton Pruitt Family Department of Biomedical Engineering

University of Florida

JG-56 Biomedical Sciences Building

1275 Center Drive

Gainesville, FL 32611-6131

E-mail: pmcfetridge@bme.ufl.edu

Received: October 1, 2012

Accepted: March 26, 2013

Online Publication Date: April 30, 2013